

Red horizontal branch stars in the Galactic field: A chemical abundance survey

M. Afşar^{1,2,a}, C. Sneden² and B.-Q. Fo³

¹*Department of Astronomy and Space Sciences, Ege University, 35100 Bornova, İzmir, Turkey*

²*Department of Astronomy and McDonald Observatory, The University of Texas, Austin, TX 78712, USA*

³*ICRAR, University of Western Australia, 35 Stirling Hwy, Crawley, WA 6009, Australia*

Abstract. A large sample survey of Galactic red horizontal-branch (RHB) stars was conducted to investigate their atmospheric parameters and elemental abundances. High-resolution spectra of 76 Galactic field stars were obtained with the 2.7 m Smith Telescope at McDonald Observatory. Only the color and the parallax were considered during the selection of the field stars. Equivalent width or synthetic spectrum analyses were used in order to determine the relative abundances of the following elements: proton-capture elements C, N, O and Li, alpha-elements Ca and Si, and neutron-capture elements Eu and La. Additionally, $^{12}\text{C}/^{13}\text{C}$ isotopic ratios were derived by using the CN features mainly located in the 7995 – 8040 spectral region. The evaluation of effective temperatures, surface gravities and $^{12}\text{C}/^{13}\text{C}$ isotopic ratios together with evolutionary stages of the candidates revealed that 18 out of 76 stars in our sample are probable RHBs. Including both kinematic and evolutionary status information, we conclude that we have five thick disk and 13 thin disk RHB stars in our sample. Although RHB stars have been regarded as thick disk members of the Galaxy, the low-velocity RHBs with a solar metallicity in our sample suggests the existence of a large number of thin disk RHBs, which cannot be easily explained by standard stellar evolutionary models.

1. INTRODUCTION

The loci of horizontal branch (HB) stars depend mainly on initial mass of the star, mass loss during the red giant branch (RGB) phase, metallicity, helium abundance, age and rotation. HB stars have a large effective temperature (T_{eff}) range. Red HB (RHB) and red clump (RC) stars, which are the coolest members of the HB, form the red end of it. RHBs are located between the instability strip and the RC stars. For RHBs, the range of color is $(B-V)_0 \approx 0.5-0.8$ [20], and the range of effective temperature is $T_{\text{eff}} \approx 5000-6200$ [9].

Kinematical and chemical abundance distributions of RHBs have been studied by several authors. [16] was the first one who investigated the field RHBs, selected among the North Galactic Pole G5-G7 stars reported by [25, 26], as a group. [16] analyzed the low resolution spectroscopic data and concluded that the RHBs are relatively metal-poor members of the Galactic “thick disk” ([7]). Later, by using RHB kinematics, [13] found their linkage with thick disk population and estimated the Galactic scale height of the thick disk as 0.6 kpc.

Some spectroscopic results indicate that the G-type RHBs are bona fide members of the thick disk. [21] obtained the high-dispersion spectra of the 10 field RHBs and concluded that the chemical compositions of RHBs are consistent with the chemical compositions of field dwarfs and red giants at

^ae-mail: melike.afsar@ege.edu.tr

similar metallicities ($-0.2 \geq [\text{Fe}/\text{H}] \geq -1.9$) so that they can be used to trace the Galactic chemical evolution. In another chemical composition study, from the detailed analysis of 13 RHBs, [22] showed that RHBs have overabundances of α -elements (O, Mg, Si, Ca, Ti) as well as of some neutron-capture elements (Eu, Zr, Sm). They also investigated the CN abundances and found a C depletion and a N enhancement in these stars, which indicate that the CN-cycle reactions are the major energy production source in the H-burning shell. Most strikingly they suggest that RHBs typically have $^{12}\text{C}/^{13}\text{C} \sim 3\text{-}6$. These values are far lower than those of thin disk Population I giants (15-25; see e.g.[14]) and “old disk” giants (10-20; [5]).

RHBs of globular clusters show a clear separation from the RGB and can be easily detected. On the other hand, it is a challenge to identify field RHBs since they can be confused with RCs or with higher-mass stars in their subgiant (SG) phase. However, it is possible to distinguish them spectroscopically from SGs which have large $^{12}\text{C}/^{13}\text{C}$ ratios and non-detectable CN surface abundance anomalies ([23]).

In this paper we report the results of a chemical abundance study of field RHB stars. We will make use of kinematics, metallicities, and chemical abundance ratios of these particular stars in order to confirm the existence of a considerable number of high-metallicity thin-disk RHB stars.

2. TARGET SELECTION AND OBSERVATIONS

We selected our program stars among the luminosity class III giants by looking mainly at their color, $(\text{B}-\text{V})_0 \approx 0.5\text{-}0.8$ (or $(\text{V}-\text{K})_0 \approx 1.5\text{-}2.2$ when possible) and spectral type (between G0 and G8). Some of the RHB candidates were chosen from the lists given by [25], [10–12] and [16]. We also made use of the SIMBAD database and the Hipparcos catalog ([27]). We were able to observe the stars with apparent magnitudes $V < 11$ due to telescope/instrumental set-up limitations.

The high-resolution, high S/N (≥ 100) spectra of the 129 RHB candidates were observed with the 2dCoude Robert G. Tull Cross-Dispersed Echelle spectrograph ([24]) of the 2.7m Harlan J. Smith Telescope at McDonald Observatory. With a spectral resolving power of $R \approx 60000$, the wavelength coverage was $\lambda\lambda$ 3400–10900. The standard data reduction procedures were carried out using IRAF¹. We were able to perform a detailed abundance analysis for the spectra of only 76 RHB candidates. The rest of the data were discarded because we could not obtain meaningful atmospheric parameters due to strong blended/broadened spectral features observed in their spectra.

3. METHOD OF ANALYSIS AND ABUNDANCES

The abundances of interest in this work were derived for 76 RHB candidates. We used two techniques: equivalent width (EW) measurements with the SPECTRE code ([6]), and spectrum synthesis by using the LTE spectral line analysis and the synthetic spectrum program MOOG ([18]).

The main stellar atmospheric parameters, i.e. of T_{eff} , $\log g$ (surface gravity), ξ_t (microturbulent velocity) and $[\text{Fe}/\text{H}]$ (metallicity), were determined by using Fe I and Fe II abundances along with model stellar atmospheres. We also derived solar abundances by applying the same procedures and used them to obtain the differential stellar abundances of our program stars.

The abundances of the α -elements Ca and Si, proton-capture elements C, N, O and Li, and neutron-capture elements of Eu and La were investigated. We used EW in order to derive Ca and Si abundances. We made use of both EW and spectrum synthesis technique to determine abundances of C (high-excitation lines and CH-G band) and O (7770 Å triplet and 6300.3 Å forbidden line). We derived abundances of N, Li, Eu and La only with the spectrum synthesis technique. Nitrogen abundances were

¹ The Image Reduction and Analysis Facility, a general purpose software package for astronomical data, is written and supported by the IRAF programming group of the National Optical Astronomy Observatory (NOAO) in Tucson, AZ, USA.

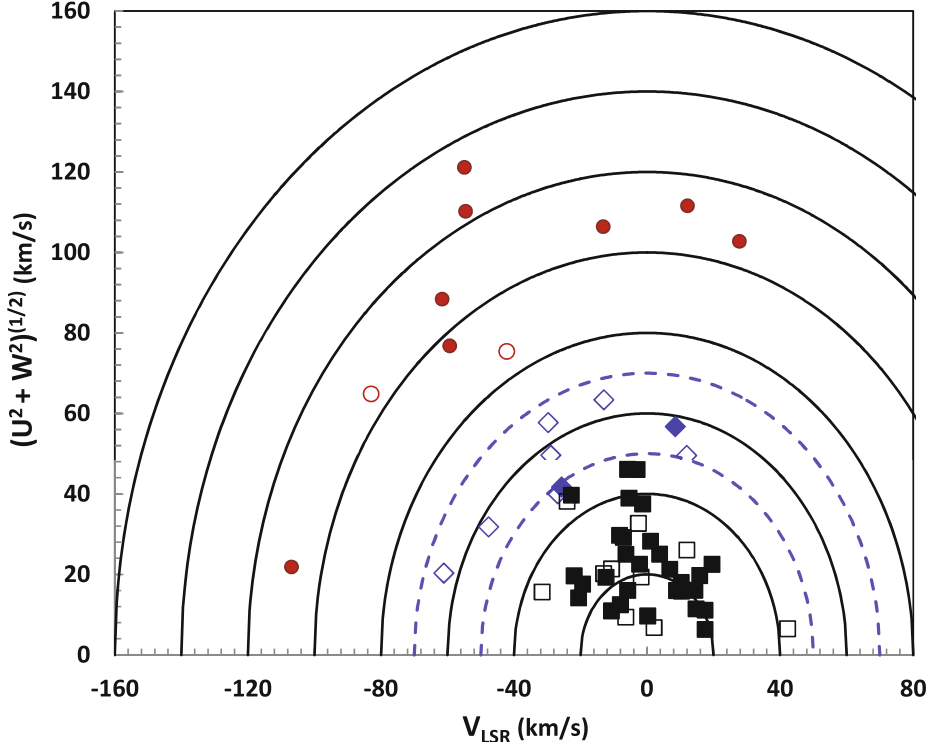


Figure 1. Toomre diagram of the program stars (adapted from Fig. 13 of [1]). Solid lines indicate V_{tot} with steps of 20 km s^{-1} . The dashed lines at 50 and 70 km s^{-1} denote the approximate thin-thick disk separation. Thin, thin/thick and thick disk stars are respectively represented by (black) squares, (blue) diamonds and (red) circles. The meaning of the filled and open symbols are explained in the text.

derived from the $7995\text{--}8040 \text{ \AA}$ region that contains strong CN features. We also determined $^{12}\text{C}/^{13}\text{C}$ isotopic ratios (one of the main issues in this study) by applying the synthetic spectrum fitting method to ^{12}CN and ^{13}CN features (see [1] for the details of the analysis technique).

4. KINEMATICS OF THE SAMPLE

Only 58 out of 76 stars of our program have distance information in the literature. We calculated the space velocities with respect to the Local Standard of Rest (LSR) for these candidates and investigated their kinematics. In Figure 1 we show a Toomre diagram for our stars. This kind of plot reveals the kinematic distribution of the stars in terms of their space velocities: U_{LSR} (positive toward the Galactic center), W_{LSR} (positive toward the North Galactic Pole), V_{LSR} (positive in the direction of the Galactic rotation). Constant total space velocities ($V_{\text{tot}} = (U_{\text{LSR}}^2 + V_{\text{LSR}}^2 + W_{\text{LSR}}^2)^{1/2}$) are represented by solid curves in the figure. The dashed line at $V_{\text{tot}} = 70 \text{ km s}^{-1}$ indicates an approximate total velocity limit for the thin-thick disk separation (e.g. [2], [15]).

The kinematic distribution of our stars shows that we have 39 probable thin disk stars (illustrated by squares in the figure, $V_{\text{tot}} < 50 \text{ km s}^{-1}$), 9 thin/thick stars which are also called transition objects (triangles, $50 < V_{\text{tot}} < 70 \text{ km s}^{-1}$) and 10 thick disk stars (circles, $70 < V_{\text{tot}} < 180 \text{ km s}^{-1}$). Filled and open symbols are used as an indication of whether ^{13}CN features were detected in individual stars. Empty symbols correspond to stars with no detection of ^{13}CN features ($^{12}\text{C}/^{13}\text{C} > 30$).

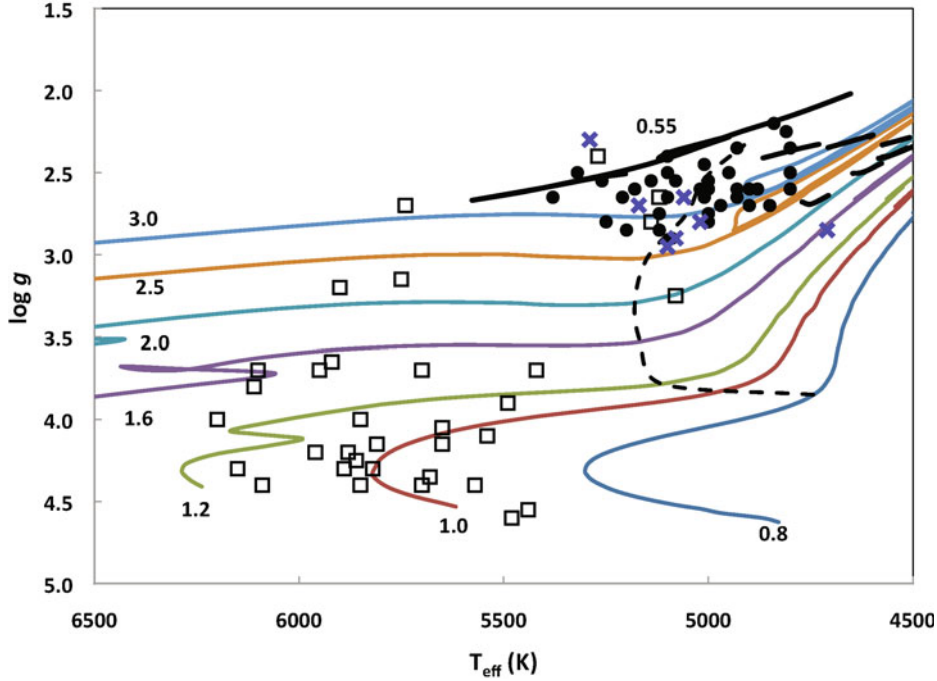


Figure 2. The spectroscopic $T_{\text{eff}}\text{-log } g$ diagram of our program stars (adapted from Fig. 17 of [1]). Stars with $^{12}\text{C}/^{13}\text{C} \leq 20$, $20 < ^{12}\text{C}/^{13}\text{C} \leq 30$ and $^{12}\text{C}/^{13}\text{C} > 30$ (no detection) are represented by filled circles, (blue) crosses and open squares, respectively. The theoretical evolutionary tracks are come from [3].

5. RESULTS

The loci of the program stars in the $T_{\text{eff}}\text{-log } g$ plane are given in Figure 2. We use different symbols for the stars with and without the detection. ^{13}CN In our sample, we have evolved stars with $20 < ^{12}\text{C}/^{13}\text{C} < 30$, which are close to the values suggested by canonical models (e.g. [17], [4]). These stars are represented by blue crosses in Figure 2.

The evaluation of the evolutionary stages of the program stars revealed that, out of 76 candidates, 18 stars of our sample are likely RHBs: 5 located in the thick disk and 13 located in the thin disk. The rest of the sample consists of RCs, RGBs, SGs and main-sequence stars.

The intriguing result of this study is that most of the RHBs in our sample are thin disk members, which have been considered as the members of the thick disk up to date. These stars are too hot ($T_{\text{eff}} > 5000$ K) to be RCs ($T_{\text{eff}} < 4900$ K), and they have surface gravities typical of evolved stars, i.e. around $\log g = 2.2\text{-}2.5$. The abundances of the α -, neutron-capture and proton-capture elements of the thin disk RHBs show no obvious inconsistencies compared to other thin disk members. They exhibit $[\text{C}/\text{Fe}] \sim -0.4$ and low $^{12}\text{C}/^{13}\text{C}$ values, which are the indicators of CNO processed material. On the other hand, the existence of thin-disk RHBs cannot be easily explained by standard stellar evolution.

In Figure 3, we investigate the possible correlation between $^{12}\text{C}/^{13}\text{C}$ ratios and $[\text{Fe}/\text{H}]$. Besides the stars we stated as plausible RHB, RC, and RC/RHB in our sample, we also include the data of those at similar stages of stellar evolution from [14], [5], [8] and [22].

A trend with metallicity is noticeable in Figure 3. This result is similar to the one previously obtained by [19]: lower metallicity RHB and RC stars have a smaller $^{12}\text{C}/^{13}\text{C}$ range than similar objects of higher metallicity. In order to be able to state that “lower metallicities have lower $^{12}\text{C}/^{13}\text{C}$ ratios”, the relation needs to be investigated in detail. The observed fluctuations in $^{12}\text{C}/^{13}\text{C}$ towards lower metallicities

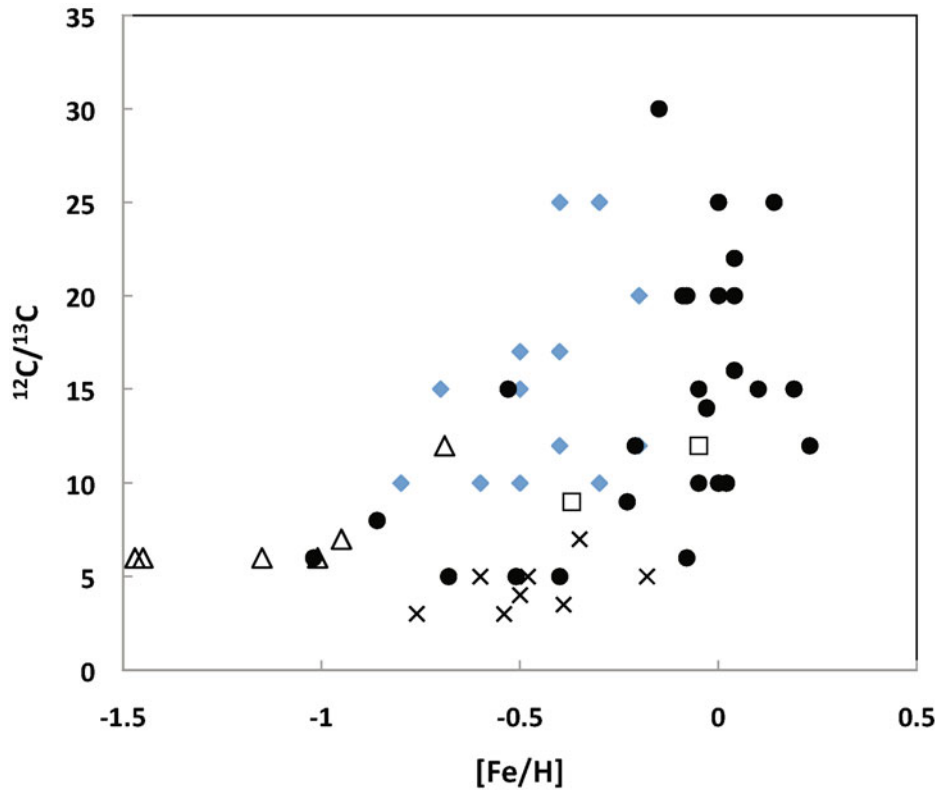


Figure 3. $^{12}\text{C}/^{13}\text{C}$ ratios (filled circles) as a function of $[\text{Fe}/\text{H}]$ for RHB, RC and RC/RHB stars (adapted from Fig. 18 of [1]). Other RCs and RHBs from [14] (open squares), [5] (grey diamonds), [8] (open triangles) and [22] (crosses) are also plotted.

might be related to mass-loss and mixing processes that the stars might have encountered during their evolution. A better understanding of mechanisms alter the CN ratio must await a significant increase in sample size of the stars who have similar evolution histories.

Our chemical abundance survey of field RHB stars resulted in a new and unexpected conclusion: the $T_{\text{eff}}\text{--}\log g$ domain of field RHBs is populated by a substantial number of high metallicity thin disk stars, which is not predicted by standard evolution studies. Our plan is to collect more data to substantially increase the field RHB sample and to investigate in detail the mechanisms that may lead RHBs to end up in this relatively rare evolutionary state.

References

- [1] Afşar, M., Sneden, C., For, B.-Q., *AJ* **144**, (2012) 20
- [2] Bensby, T. & Feltzing, S., in *Chemical Abundances in the Universe: Connecting First Stars to Planets*, IAUS **265**, (2010) 300
- [3] Bertelli, G., Girardi, L., Marigo, P. & Nasi, E., *A&A*, **484**, (2008) 815
- [4] Charbonnel, C., *A&A* **282**, (1994) 811
- [5] Cottrell, P. L., & Sneden, C., *A&A* **161**, (1986) 314
- [6] Fitzpatrick, M. J., & Sneden, C., *BAAS* **19**, (1987) 1129
- [7] Gilmore, G., & Reid, N., *MNRAS* **202**, (1983) 1025
- [8] Gratton, R. G., Sneden, C., Carretta, & E., Bragaglia, A., *A&A* **354**, (2000) 169

- [9] Gray, R. O., & Corbally, C. J., *Stellar Spectral Classification* (Princeton: Princeton University Press, 2009)
- [10] Harlan, E. A., *AJ* **74**, (1969) 916
- [11] Harlan, E. A., *AJ* **79**, (1974) 682
- [12] Harlan, E. A., *AJ* **86**, (1981) 1896
- [13] Kaempf, T. A., de Boer, K. S., & Altmann, M., *A&A* **432**, (2005) 879
- [14] Lambert, D. L., & Ries, L. M., *ApJ* **248**, (1981) 228
- [15] Nissen, P. E., in *Origin and Evolution of the Elements* (Carnegie Observatories Astrophysics Series **Vol. 4**, (Eds.) A. McWilliam and M. Rauch, Pasadena: Carnegie Observatories, 2004) p. 154
- [16] Rose, J. A., *AJ* **90**, (1985) 787
- [17] Schaller, G., Schaerer, D., Meynet, G., & Maeder, A., *A&AS* **96**, (1992) 269
- [18] Sneden, C., *ApJ* **184**, (1973) 839
- [19] Sneden, C., *Evolution of Stars: the Photospheric Abundance Connection*, *IAUS* **145**, (1991) 235
- [20] Straizys, V., Bartkevicius, A., & Sperauskas, J., *A&A* **99**, (1981) 152
- [21] Tautvaišienė, G., *MNRAS* **286**, (1997) 948
- [22] Tautvaišienė, G., Edvardsson, B., Tuominen, I., & Ilyin, I., *A&A* **380**, (2001) 578
- [23] Thorén, P., Edvardsson, B., & Gustafsson, B., *A&A* **425**, (2004) 187
- [24] Tull, R. G., MacQueen, P. J., Sneden, C., & Lambert, D. L., *PASP* **107**, (1995) 251
- [25] Uggren, A. R., *AJ* **67**, (1962) 37
- [26] Uggren, A. R., *AJ* **68**, (1963) 194
- [27] van Leeuwen, F., *A&A* **474**, (2007) 653